Open Access Journal

Indian Journal of Medical Research and Pharmaceutical Sciences

August 2016 3(8) ISSN: ISSN: 2349-5340

DOI: 10.5281/zenodo.59821 Impact Factor: 3.052

HUHS1015 PROMOTES AUTOPHAGIC XIAP DEGRADATION TO INDUCE APOPTOSIS OF GASTROINTESTINAL CANCER CELLS

Tomoyuki Nishizaki*

*Innovative Bioinformation Research Organization, Kobe, Japan

Keywords:

Gastrointestinal cancer cell, Apoptosis, Caspase-3, XIAP Autophagy

Abstract

The present study aimed at understanding the mechanism underlying HUHS1015-induced apoptosis of MKN45 gastric cancer and Caco-2 colonic cell, Apoptosis, cancer cell lines. HUHS1015 apparently reduced presence of mRNA protein of X-linked inhibitor of apoptosis protein (XIAP) in a treatment time Autophagy (10-60 min)-dependent manner.

The reduction of XIAP protein was prevented by the autophagy inhibitors 3-methyladenine and bafilomycin A1. XIAP knock-down significantly activated caspase-3 and reduced cell viability in MKN45 and Caco-2 cells. In the flow cytometry using propidium iodide (PI) and annexin V-FITC (AV), XIAP knock-down significantly increased the proportions of PI-positive/AV-negative, PI-negative/AV-positive, and PI-positive/AV-positive cells, which corresponds to primary necrosis, early apoptosis, and late apoptosis/secondary necrosis, respectively, in both the cell lines. Taken together, the results of the present study indicate that HUHS1015 promotes autophagic XIAP degradation in MKN45 and Caco-2 cells, thereby neutralizing caspase-3 inhibition due to XIAP, to activate caspase-3 and induce apoptosis.

Introduction

The newly synthesized anticancer drug 1-[2-(2-methoxyphenylamino) ethylamino]-3-(naphthalene-1-yloxy)propan-2-ol (HUHS1015) induces apoptosis of a variety of cancer cell lines including human gastric cancer cell lines MKN28 and MKN45 cells, and the mechanisms underlying HUHS1015-induced apoptosis differ, depending upon cancer cell types [1-5]. HUHS1015 induced apoptosis of MKN28 cells by accumulating apoptosis-inducing factor (AIF) homologous mitochondrion-associated inducer of death (AMID) in the nucleus [3.5]. HUHS1015, alternatively, induced apoptosis of MKN45 cells in part by activating caspase-8 through tumor necrosis factor (TNF) receptor in association with upregulation of TNFα [4,5]. Amazingly, huge activation of caspase-3 was induced by HUHS1015, the maximum reaching over 15 folds higher than that for caspase-8 [4]. This suggests that HUHS1015-induced caspase-3 activation is not induced by only caspase-8; in other words, the additional pathways underlie HUHS1015-induced caspase-3 activation in MKN45 cells. HUHS1015-induced huge casapase-3 activation is also obtained with human colonic cancer cell lines Caco-2 and CW2 cells.

Caspase-3 is activated through proteolytic processing due to caspase-4, -8, or -9. Exhaustion of calcium in the endoplasmic reticulum (ER) induces ER stress and simultaneously activates the calcium-dependent, non-lysosomal cysteine protease calpain, to activate caspase-4 [6]. Caspase-8 is activated through death receptors such as Fas and TNF receptors [7]. Mitochondrial damage releases cytochrome c, which forms a complex with an apoptotic protease activating factor 1 (Apaf-1)/dATP, to activate caspase-9 [8]. Moreover, mitochondrial damage releases other apoptosis-related factors such as Smac/DIABLO. Smac/DIABLO, a X-linked inhibitor of apoptosis protein (XIAP) binding protein, is released from damaged mitochondria and antagonizes caspase-3 inhibition due to XIAP [9]. Caspase-3 is also activated by relief from inhibition due to XIAP, regardless of upstream caspase-4, -8, and -9

Indian Journal of Medical Research and Pharmaceutical Sciences
August 2016 3(8) ISSN: ISSN: 2349-5340
DOI: 10.5281/zenodo.59821 Impact Factor: 3.052

[10]. In the present study, we show that HUHS1015 activates caspase-3 in gastrointestinal cancer cell lines MKN45 and Caco-2 cells by promoting autophagic XIAP degradation.

Materials and Methods

Cell culture

MKN45 and Caco-2 cells were grown in RPMI-1640 medium and Dulbecco's modified Eagle's medium, supplemented with 10% (v/v) heat-inactivated fetal bovine serum, penicillin (final concentration, 100 U/ml) and streptomycin (final concentration, 0.1 mg/ml) in a humidified atmosphere of 5% CO_2 and 95% air at 37 °C.

Real-time reverse transcription-polymerase chain reaction (RT-PCR)

Real-time RT-PCR was carried out using the following primers: for *XIAP*, sense; TATTGCTATCGTTTTTGTTCCTTGTGGA and anti-sense; AAATGGACAGAATCCTAAAACACAACAACC and for *GAPDH*, sense; GACTTCAACAGCGACACCCACTCC and anti-sense; AGGTCCACCACCCTGTTGCTGTAG. Total RNAs were purified from cells using a Sepasol-RNA I Super kit (Nacalai, Kyoto, Japan) and treated with RNase-free DNase I (2 units) at 37 °C for 30 min. Then, random primers, dNTP, 10× RT buffer, and Multiscribe Reverse Transcriptase were added to the RNA solution and incubated at 25 °C for 10 min followed by 37 °C for 120 min to synthesize the first-strand cDNA. Real-time RT-PCR was performed using a SYBR Green Realtime PCR Master Mix (Takara Bio, Otsu, Japan) and the Applied Biosystems 7900 real-time PCR detection system (ABI, Foster City, CA). Thermal cycling conditions were as follows: first step, 94 °C for 4 min; the ensuing 40 cycles, 94 °C for 1 s, 65 °C for 15 s, and 72 °C for 30 s. The expression level of the XIAP mRNA was normalized by that of GAPDH mRNA.

Western blotting

Samples were loaded on 10% (v/v) sodium dodecyl sulfate-poly acrylamide gel electrophoresis (SDS-PAGE) and transferred to polyvinylidene difluoride membrane. After blocking with TBST [20 mM Tris, 150 mM NaCl, 0.1 % (v/v) Tween-20, pH 7.5] containing 5% (w/v) of bovine serum albumin, blotting membrane was reacted with an antibody against XIAP (Santa Cruz Biotechnology, Inc., Dallas, Texas, USA) and β-actin (SIGMA, Missouri, SL, USA), followed by a horseradish peroxidase (HRP)-conjugated anti-mouse IgG antibody. Immunoreactivity was detected with an ECL kit (Invitrogen, Carlsbad, CA, USA) and visualized using a chemiluminescence detection system (GE Healthcare, Piscataway, NJ, USA). Protein concentrations for each sample were determined with a BCA protein assay kit (Thermo Fisher Scientific, Rockford, IL, USA).

Construction and transfection of siRNA

The siRNA to silence the XIAP-targeted gene (5'-GGAUAUACUCAGUUAACAAtt-3' and 5'-UUGUUAACUGAGUAUAUCCat-3') was obtained from Invitrogen (Carlsbad, CA, USA) and the negative control (NC) siRNA, which has the scrambled sequence, and the GC content and nucleic acid composition same as those for the XIAP siRNA was from Inveitrogen. siRNAs were transfected into cells using a Lipofectamine reagent, and cells were used for experiments 48 h after transfection.

Cell viability

Cell viability was evaluated by the method using 3-(4,5-dimethyl-2-thiazolyl)-2,5-diphenyl-2H-tetrazolium bromide (MTT).

Flow cytometry

Cells, which were stained with both propidium iodide (PI) and annexin V-FITC (AV), were loaded on a flow cytometer (FACSCalibur) available for FL1 (AV) and FL2 (PI) bivariate analysis. Data from 10,000 cells/sample were collected, and the quadrants were set according to the population of viable, unstained cells in untreated samples. CellQuest analysis of the data was used to calculate the percentage of the cells in the respective quadrants.

Enzymatic assay of caspase activity

Caspase activity was measured using a caspase fluorometric assay kit: Ac-Asp-Glu-Val-Asp-MCA for a caspase-3 substrate peptide, Ac-Leu-Glu-Val-Asp-AFC for a caspase-4 substrate peptide, Ac-Ile-Glu-Thr-Asp-MCA for a caspase-8 substrate peptide, and Ac-Leu-Glu-His-Asp-MCA for a caspase-9 substrate peptide. Briefly, cells were

August 2016 3(8) ISSN: ISSN: 2349-5340
DOI: 10.5281/zenodo.59821 Impact Factor: 3.052

harvested before and after treatment with HUHS1015, and then centrifuged at 800 *g* for 5 min at 4 °C. The pellet was incubated on ice in cell lysis buffer for 10 min, and then centrifuged at 10,000 *g* for 1 min at 4 °C. The supernatant was reacted with the fluorescently labeled tetrapeptide at 37 °C for 2 h. Fluorescence was measured at an excitation wavelength of 380 nm and an emission wavelength of 460 nm for caspase-3, -8, and -9 or at an excitation wavelength of 400 nm and an emission wavelength of 505 nm for caspase-4 with a fluorescence microplate reader (TECAN Infinite, Männedorf, Switzerland).

Statistical analysis

Statistical analysis was carried out using analysis of variance (ANOVA) followed by a Bonferroni correction and unpaired *t*-test.

Results

In the real-time RT-PCR, HUHS1015 reduced presence of the XIAP mRNA in MKN45 and Caco-2 cells in a treatment time (10-60 min)-dependent manner (Figure 1A,B). In the Western blot analysis, HUHS1015 reduced presence of XIAP protein as well in both the cell lines in a treatment time (10-60 min)-dependent manner (Figure 1C,D). Considering reduction of the mRNA and protein within 60 min, the effect of HUHS1015 would not be due to inhibition of transcription or translation. Then, we postulated that HUHS1015 might reduce presence of XIAP by promoting XIAP degradation.

To address this point, we examined the effect of HUHS1015 using the proteasome inhibitor MG132. HUHS1015-induced reduction of XIAP protein in MKN45 cells was not affected by MG132 (Figure 2). This rules out the possibility for proteasomal degradation of ubiquitin-conjugated XIAP.

In contrast, HUHS1015-induced reduction of XIAP protein was significantly prevented by 3-methyladenine (3-MA), an inhibitor of phosphoinositide 3-kinase (PI3K) bearing regulator of the initial autophagy, in MKN45 and Caco-2 cells (Figure 3A,B). In addition, the effect of HUHS1015 was also inhibited by bafilomycin A1 (BA1), an inhibitor of the late-phase autophagy, in both the cell lines (Figure 3C,D). Collectively, these results indicate that HUHS1015 promotes autophagic XIAP degradation in MKN45 and Caco-2 cells.

The expression levels of XIAP protein in MKN45 and Caco-2 cells transfected with the XIAP siRNA were definitely decreased as compared with those for cells transfected with the NC siRNA (Figure 4A,B), confirming successful XIAP knock-down.

Activity of caspase-3 in MKN45 and Caco-2 cells was significantly enhanced by knocking-down XIAP as compared with that in cells transfected with the NC siRNA (Figure 5A,B). XIAP knock-down also activated caspase-4, -8, and -9 in Caco-2 cells, while no significant activation of these caspases was obtained with MKN45 cells (Figure 5A,B).

In the MTT assay, cell viability for MKN45 and Caco-2 cells was reduced by knocking-down XIAP (Figure 5C,D).

In the flow cytometry, XIAP knock-down significantly increased the proportions of PI-positive/AV-negative, PI-negative/AV-positive, and PI-positive/AV-positive cells and decreased the proportion of PI-negative and AV-negative cells both in MKN45 and Caco-2 cells as compared with those for cells without XIAP knock-down (Figure 5A,B). This indicates that primary necrosis, early apoptosis, and late apoptosis/secondary necrosis are induced by knocking-down XIAP. Overall, these results interpret that reduction of XIAP protein is responsible for activation of caspase-3 and induction of apoptosis of MKN45 and Caco-2 cells.

Discussion

We have earlier found that HUHS1015 induces caspase-dependent apoptosis of MKN45 human poorly differentiated gastric adenocarcinoma cell line, but not MKN28 well-differentiated gastric adenocartinoma cell line, with drastic activation of caspase-3 [4]. The mechanism of HUHS1015-induced caspase-3 activation, however, remained to be elucidated. Caspase-3 is a downstream effector caspase of caspase-4, -8, and -9, but HUHS1015

August 2016 3(8) ISSN: ISSN: 2349-5340
DOI: 10.5281/zenodo.59821 Impact Factor: 3.052

induced less/little activation of caspase-4, -8, and -9 in MKN45 and Caco-2 cells [11]. This suggests that HUHS1015 activates caspase-3 though a pathway independent of caspase-4, -8, and -9.

Intriguingly, HUHS1015 reduced presence of the XIAP mRNA and protein in MKN45 and Caco-2 cells. XIAP serves as an inhibitor of caspase-3 [10]. Reduction of XIAP, therefore, could neutralize caspase-3 inhibition due to XIAP, allowing caspase-3 activation. Surprisingly, the effect of HUHS1015 was found within 60-min treatment time. This indicates that HUHS1015-induced reduction of the XIAP mRNA and protein is not due to suppression of transcription and translation. HUHS1015-induced reduction of XIAP protein was the autophagy inhibitors 3-MA and BA1. Overall, these results lead to a conclusion that HUHS1015 promotes autophagic XIAP degradation, thereby neutralizing caspase-3 inhibition due to XIAP, to activate caspase-3 and induce apoptosis of MKN45 and Caco-2 cells. In further support of this conclusion, caspase-3 activation and apoptotic cell death in MKN45 and Caco-2 cells were induced by knocking-down XIAP.

Cell death is classified into necrosis and programmed cell death, and the latter includes apoptosis, necroptosis, and autophagic death [12]. Autophagic cell death is related to autophagy. Autophagy is a self-cannibalization machinery bearing the engulfment of cytoplasmic material and intracellular organelles within a double-membrane vesicle, so called autophagosome. Autophagosome is fused with lysosome, to form autolysosome, where the captured materials are degraded by specific acidic hydrolases [13].

Starvation, stress, hypoxia, glucagons, and depletion of growth factors and amino acids are recognized to activate autophagy [14]. These factors inactivate mammalian target of rapamycin complex 1 (mTORC1), to recruit core autophagy-related proteins such as Atg1/Atg13/Atg17/Atg29/Atg31 for organization of pre-autophagosomal structure (PAS)[14]. Conversely, activation of mTROC1 phosphorylates Atg13, to prevent recruitment of Atg proteins [15]. A complex of Atg1/Atg13/Atg17/Atg29/Atg31 activates PI3K complex I, which is composed of Atg14/Atg15/Atg30/Atg34, to produce phosphatidylinositol (3,4,5)-triphosphate [PI(3,4,5)P_3] at the PAS and recruit the PI(3,4,5)P_3-binding protein Atg18 and its associated protein Atg2 [15]. PI3K complex I, alternatively, makes the Atg8-phosphatidylethanolamine (PE) and Atg12-Atg5 conjugates [15]. Atg4 cleaves the arginine residue of Atg8 to expose the glycine residue and in turn, Atg8 is activated by Atg7 (an E1 enzyme), transferred to Atg3 (an E2 enzyme) and eventually conjugated to PE [15]. Atg4 also cleaves the amide bond between Atg8 and PE to release the protein from membranes [15]. Atg12 is still activated by Atg7 and transferred to Atg10 (an E2 enzyme), and then, Atg12 is conjugated to the lysine residue of Atg5 [15]. The Atg12-Atg5 conjugate interacts with Atg16 and the complex of Atg12/Atg5/Atg16 exerts an E3 enzyme-like action on the transfer reaction of Atg8 from Atg3 to PE [15]. The Atg8-PE conjugate and the Atg12/Atg5/Atg16 complex play a critical role in all the processes of autophagy [15].

Mouse double minute 2 homolog (Mdm2) serves as an E3 ubiquitin ligase, to promote proteosomal degradation of the tumor suppressor p53, and an inhibitor of p53 transcription. Amazingly, emerging evidence has pointed to XIAP as an E3 ubiquitin ligase for Mdm2 [16,17]. When phosphorylated by Akt, XIAP promotes ubiqutination and proteasomal degradation of caspase-3, -7, and -9, resulting in resistance to apoptosis. Phosphorylated XIAP, alternatively, promotes ubiqutination and proteasomal degradation of Mdm2, thereby preventing proteosomal degradation of p53 and stabilizing cytosolic p53 [16,17]. Cytosolic p53 acts as a repressor of autophagy, while nuclear p53 promotes the transcriptional activation of autophagy-related genes [18,19]. Phosphorylated XIAP, therefore, suppresses autophagy resulting from stabilization of cytosolic p53. In contrast, unphosphorylated XIAP allows Mdm2-mediated ubiqutination and proteasomal degradation of p53, leading to stimulation of autophagy. Phosphorylation of XIAP at Ser87 due to Akt or protein kinase C is shown to suppress apoptotic cell death by inhibiting ubiquitination and proteosomal degradation of XIAP [20,21]. Conversely, a mutant XIAP deleting the Ser87 phosphorylation site is rapidly degraded and cisplatin induces apoptosis of cells with the mutant XIAP, with the potential greater than that for cells with wild-type XIAP [20]. In the present study, HUHS1015-induced degradation of XIAP was not inhibited by the proteasome inhibitor MG132. In addition, HUHS1015 did not affect the serine phosphorylation levels of XIAP in MKN45 cells (data not shown). Collectively, these results exclude the possibility that HUHS1015 promotes proteosomal degradation of XIAP by reducing serine phosphorylation of

August 2016 3(8) ISSN: ISSN: 2349-5340
DOI: 10.5281/zenodo.59821 Impact Factor: 3.052

XIAP. It is presently unknown how HUHS1015 promotes autophagic XIAP degradation. To address this question, we are currently testing further experiments.

Conclusion

The results of the present study show that HUHS1015 promotes autophagic XIAP degradation in MKN45 and Caco-2 cells (Figure 6), resulting in the reduced intracellular XIAP levels, which allows activation of caspase-3 in association with relief from caspase-3 inhibition due to XIAP, to induce apoptosis. This may represent further insight into the mechanism underlying HUHS1015-induced apoptotic cell death.

Conflict of interests

We have no conflict of interests.

References

1. Kanno T, Tanaka A, Shimizu T, Nakano T, Nishizaki T. 1-[2-(2-Methoxyphenylamino)ethylamino]-3-(naphthalene-1-yloxy)propan-2-ol as a potential anticancer drug. Pharmacology 2013;91 (5-6):339-345.
2. Kaku Y, Nagaya H, Tsuchiya A, Kanno T, Gotoh A, Tanaka A, Shimizu T, Nakao S, Tabata C, Nakano T, Nishizaki T. Newly synthesized anticancer drug HUHS1015 is effective on malignant pleural mesothelioma. Cancer Sci 2014;105(7): 883-889.
3. Kaku Y, Tsuchiya A, Kanno T, Nishizaki T. HUHS1015 induces necroptosis and caspase-independent apoptosis of MKN28 human gastric cancer cells in association with AMID accumulation in the nucleus. Anticancer Agents Med Chem 2015;15(2):242-247.
4. Kaku Y, Tsuchiya A, Kanno T, Nakao S, Shimizu T, Tanaka A, Nishizaki T. The newly synthesized anticancer drug HUHS1015 is useful for treatment of human gastric cancer. Cancer Chemother Pharmacol 2015;75(3):527-535.
5. Nishizaki T, Kanno T, Tsuchiya A, Kaku Y, Shimizu T, Tanaka A. 1-[2-(2-Methoxyphenylamino)ethylamino]-3-(naphthalene-1-yloxy)propan-2-ol may be a promising anticancer drug. Molecules 2014;19(12):21462-21472.
6. Matsuzaki S, Hiratsuka T, Kuwahara R, Katayama T, Tohyama M. Caspase-4 is partially cleaved by calpain via the impairment of Ca^{2+} homeostasis under the ER stress. Neurochem Int 2010;56(2):352-356.
7. Muzio M. Signalling by proteolysis: death receptors induce apoptosis. Int J Clin Lab Res 1998;28(3):141-147.
8. Kuida K. Caspase-9. Int J Biochem Cell Biol 2000;32(2):121-124.
9. Vaux DL, Silke J. Mammalian mitochondrial IAP binding proteins. Biochem Biophys Res Commun 2003;304(3):499-504.
10. Gao Z, Tian Y, Wang J, Yin Q, Wu H, Li YM, Jiang X. A dimeric Smac/diablo peptide directly relieves caspase-3 inhibition by XIAP. Dynamic and cooperative regulation of XIAP by Smac/Diablo. Biol Chem 2007;282(42): 30718-30727.
11. Kaku Y, Tsuchiya A, Shimizu T, Tanaka A, Nishizaki T. HUHS1015 suppresses colonic cancer growth by inducing necrosis and apoptosis in association with mitochondrial damage. Anticancer Res 2016;36(1):39-48.
12. Nikoletopoulou V, Markaki M, Palikaras K, Tavernarakis N. Crosstalk between apoptosis, necrosis and autophagy. Biochim Biophys Acta 2013;1833(12): 3448-3459.
13. Levine B, Kroemer G. Autophagy in the pathogenesis of disease. Cell 2008;132(1):27-42.
14. Li X, Xu HL, Liu YX, An N, Zhao S, Bao JK. Autophagy modulation as a target for anticancer drug discovery. Acta Pharmacol Sin 2013;34(5):612-624.
15. Nakatogawa H, Suzuki K, Kamada Y, Ohsumi Y. Dynamics and diversity in autophagy mechanisms: lessons from yeast. Nat Rev Mol Cell Biol 2009;10(7): 458-467.
16. Huang X, Wu Z, Mei Y, Wu M (2013) XIAP inhibits autophagy via XIAP-Mdm2-p53 signalling. EMBO J 2013;32(16):2204-2216.
17. Merlo P, Cecconi F. XIAP: inhibitor of two worlds. EMBO J 32(16): 2187-2188.
18. Tasdemir E, Chiara Maiuri M, Morselli E, Criollo A, D'Amelio M, Djavaheri-Mergny M, Cecconi F, Tavernarakis N, Kroemer G. A dual role of p53 in the control of autophagy. Autophagy 2008;4(6):810-814.

Indian Journal of Medical Research and Pharmaceutical Sciences
August 2016 3(8) ISSN: ISSN: 2349-5340
DOI: 10.5281/zenodo.59821 Impact Factor: 3.052

19. Tasdemir E, Maiuri MC, Galluzzi L, Vitale I, Djavaheri-Mergny M, D'Amelio M, Criollo A, Morselli E, Zhu C, Harper F, Nannmark U, Samara C, Pinton P, Vicencio JM, Carnuccio R, Moll UM, Madeo F, Paterlini-Brechot P, Rizzuto R, Szabadkai G, Pierron G, Blomgren K, Tavernarakis N, Codogno P, Cecconi F, Kroemer G. Regulation of autophagy by cytoplasmic p53. Nat Cell Biol 2008;10(6):676-687.
20. Dan HC, Sun M, Kaneko S, Feldman RI, Nicosia SV, Wang HG, Tsang BK, Cheng JQ. Akt phosphorylation and stabilization of X-linked inhibitor of apoptosis protein (XIAP). J Biol Chem 2004;279(7):5405-5412.
21. Kato K, Tanaka T, Sadik G, Baba M, Maruyama D, Yanagida K, Kodama T, Morihara T, Tagami S, Okochi M, Kudo T, Takeda M. Protein kinase C stabilizes X-linked inhibitor of apoptosis protein (XIAP) through phosphorylation at Ser^{87} to suppress apoptotic cell death. Psycogeriatrics 2011;11(2):90-97.

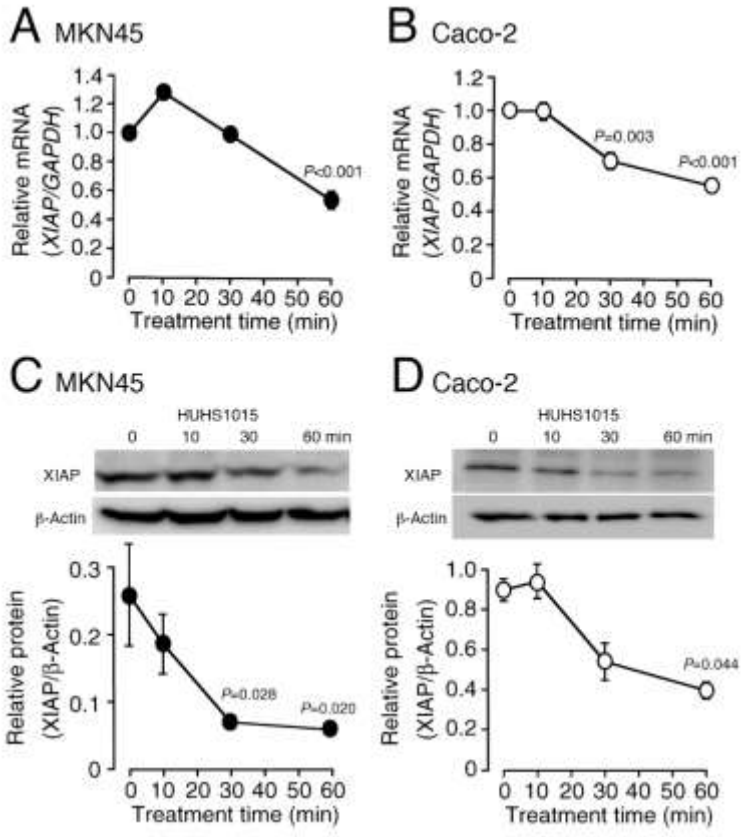

Figure 1. ***HUHS1015 reduces presence of the XIAP mRNA and protein in MKN45 and Caco-2 cells.***

Cells were treated with HUHS1015 (100 μM) for periods of time as indicated, followed by real time RT-PCR and Western blotting. (**A**,**B**) Each point represents the mean (± SEM) XIAP mRNA level normalized by the GAPDH mRNA level in MKN45 (**A**) and Caco-2 cells (**B**) (n=4 independent experiments). (**C**,**D**) In the graphs, each point represents the mean (± SEM) XIAP protein level relative to the β-actin level in MKN45 (**C**) and Caco-2 cells (**D**) (n=4 independent experiments). *P* values as compared with the values at 0-min treatment, ANOVA followed by a Bonferroni correction.

Indian Journal of Medical Research and Pharmaceutical Sciences
August 2016 3(8) ISSN: ISSN: 2349-5340
DOI: 10.5281/zenodo.59821 Impact Factor: 3.052

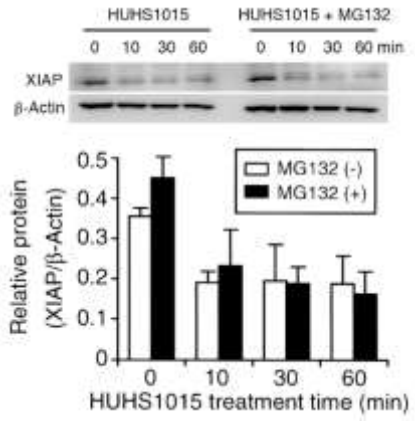

Figure 2. ***HUHS1015-induced reduction of XIAP protein is not due to proteasomal degradation.***

MKN45 cells treated with HUHS1015 (100 μM) in the presence and absence of MG132 (40 μM) for periods of time as indicated, followed by Western blotting. In the graph, each column represents the mean (± SEM) XIAP protein level relative to the β-actin level (n=4 independent experiments).

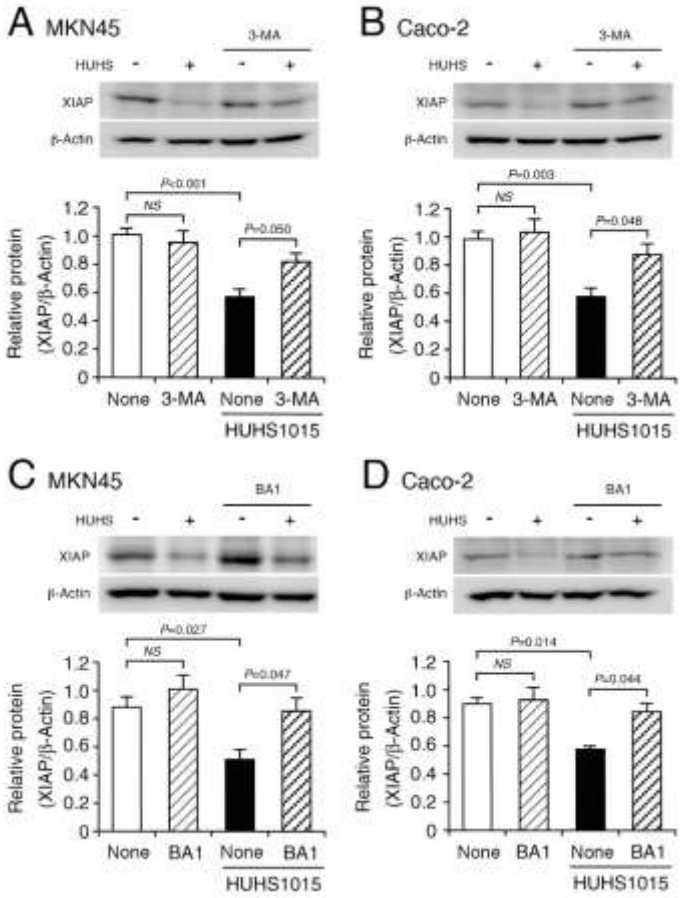

Figure 3. ***HUHS1015-induced reduction of XIAP protein is due to autophagic degradation.***

Indian Journal of Medical Research and Pharmaceutical Sciences
August 2016 3(8) ISSN: ISSN: 2349-5340
DOI: 10.5281/zenodo.59821 Impact Factor: 3.052

MKN45 (**A**,**C**) and Caco-2 cells (**B**,**D**) were treated with HUHS1015 (50 μM) in the presence and absence of 3-MA (10 mM) or BA1 (1 μM) for 30 min, followed by Western blotting. In the graphs, each column represents the mean (± SEM) XIAP protein level relative to the β-actin level (n=4-8 independent experiments). *P* values, ANOVA followed by a Bonferroni correction.

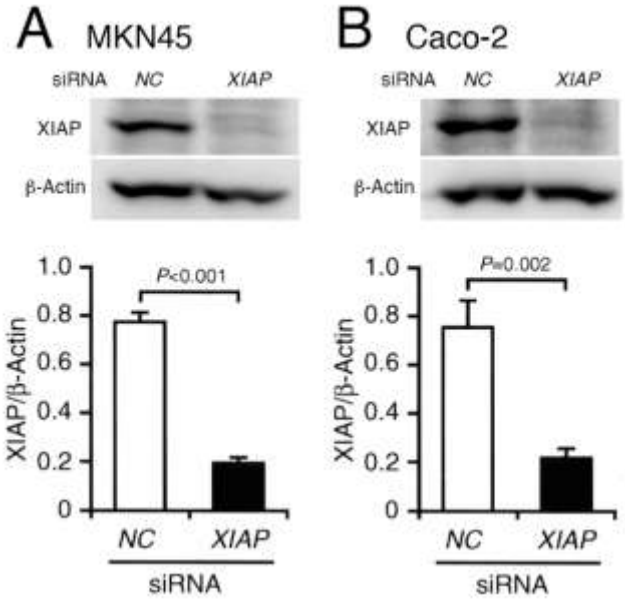

Figure 4. ***XIAP knock-down.***

The NC or XIAP mRNA was transfected into MKN45 (**A**) and Caco-2 cells (**B**), and 48 h later Western blotting was carried out. In the graph, each column represents the mean (± SEM) XIAP protein level relative to the β-actin level (n=4 independent experiments). *P* values, unpaired *t*-test.

Indian Journal of Medical Research and Pharmaceutical Sciences
August 2016 3(8) ISSN: ISSN: 2349-5340
DOI: 10.5281/zenodo.59821 Impact Factor: 3.052

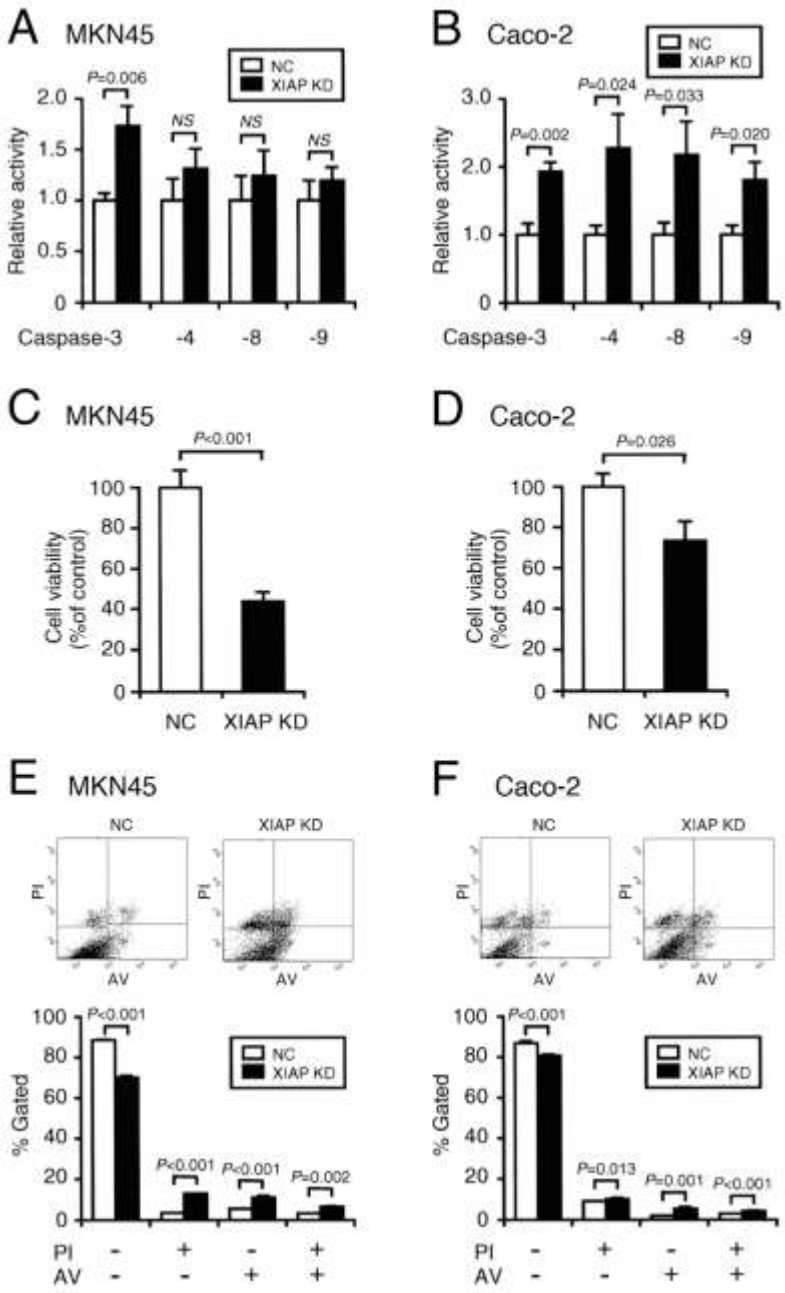

Figure 5. ***XIAP knock-down activates caspase-3, reduces cell viability, and induces apoptosis.***

The NC or XIAP siRNA was transfected into MKN45 (**A**,**C**,**E**) and Caco-2 cells (**B**,**D**,**E**), and 48 h later enzymatic caspase assay, MTT assay, and flow cytometry were carried out. (**A**,**B**) In the graphs, each column represents the mean (± SEM) caspase activity in cells transfected with the XIAP siRNA relative to that in cells with the NC siRNA (n=4 independent experiments). *P* values, unpaired *t*-test. *NS*, not significant. (**C**,**D**) In the graphs, each column represents the mean (± SEM) viability of cells transfected with the XIAP siRNA relative to that of cells with the NC siRNA (n=4 independent experiments). *P* values, unpaired *t*-test. (**E**,**F**) In the graphs, each column represents the mean (± SEM) proportion of PI-negative (-)/AV-negative (-) PI-positive (+)/AV-negative (-), PI-negative (-)/AV-

Indian Journal of Medical Research and Pharmaceutical Sciences
August 2016 3(8) ISSN: ISSN: 2349-5340
DOI: 10.5281/zenodo.59821 Impact Factor: 3.052

positive (+), or PI-positive (+)/AV-positive (+) cells for cells transfected with the XIAP siRNA relative to that for cells with the NC siRNA (n=4 independent experiments). *P* values, unpaired *t*-test. *NS*, not significant.

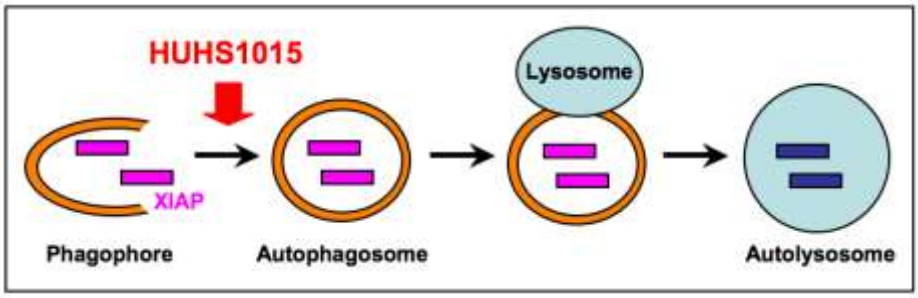

Figure 6. ***HUHS1015-induced autophagic degradation of XIAP.***